

Gaillard N, Williams-Jones AE, Clark JR, Salvi S, Beziat D, Lypaczewski P, Perrouty S, Linnen RL, 2015, Mineralogical and geochemical vectors to ore: the alteration halo of the Canadian Malartic gold deposit, Extended abstract, Society for Geology Applied to Mineral Deposits (SGA), Nancy, France, 2, 461-464

NSERC-CMIC Mineral Exploration Footprints Project Contribution 047.

Mineralogical and Geochemical Vectors to Ore: the Alteration Halo of the Canadian Malartic Gold Deposit

Nicolas Gaillard, Anthony E Williams-Jones, James R Clark

Department of Earth and Planetary Sciences, McGill University, Montréal, Canada - nicolas.gaillard@mail.mcgill.ca

Stefano Salvi, Didier Béziat

GET, CNRS, University of Toulouse, France

Philip Lypaczewski

Department of Earth and Atmospheric Sciences, University of Alberta, Edmonton, Canada

Stéphane Perrouty, Robert L Linnen

Department of Earth Sciences, University of Western Ontario, London, Canada

Abstract. Canadian Malartic is a large-tonnage, low-grade gold deposit located in the Pontiac Subprovince (southern Superior Province) immediately south of the Cadillac-Larder Lake fault zone, marking the boundary with the Abitibi Subprovince. Gold occurs mainly as disseminated grains of native gold and gold-tellurides in altered (K-feldspar-biotite-carbonates-pyrite) quartz monzodiorite porphyries and adjacent metasedimentary rocks (greywacke and siltstone). In metagreywacke, there are pronounced gains in major elements such as K, Na, Ca in samples from the ore shell (the same is true for LOI). Significantly, C and S, as well as trace elements associated with mineralization (e.g., Mo, Sb, As, W, Pb, Te and Ag), exhibit mass gains of several orders of magnitude compared to least altered equivalents. Some of these elements display trends of steadily decreasing concentration toward the distal parts of the halo. Biotite and white mica in the metasedimentary rocks exhibit chemical gradients from unaltered rocks (higher metamorphic grade) toward the deposit and their compositions represent potentially important vectoring tools. Significantly, micas from the deposit are characterized by higher Fe and Mg concentrations than those distal from mineralization. In the case of white mica, there is a steady trend from phengitic muscovite toward end-member muscovite southwards from the deposit.

Keywords. Gold, alteration halo, ore vectoring, mass changes, mineral chemistry, biotite, white mica

1 Geological context

The Canadian Malartic gold deposit (8.94 Moz at 1.06 g/t Au reserves, 5.55 Moz Au historic production) is hosted mainly by Pontiac Group metaturbidites (greywacke/siltstone, ~2685±3 Ma; Davis 2002) and porphyritic quartz monzodiorite stocks (emplaced at 2677-2679 Ma, Clark et al. in prep.; De Souza et al. 2014) intruding Piché and Pontiac group rocks. In the northeast part of the deposit (Barnat and East Malartic orebodies), a volumetrically smaller part of the mineralization occurs in ultramafic/mafic schistose volcanic rocks of the Piché Group (komatiites and basalts).

The metamorphic grade is currently interpreted to increase southward from greenschist to amphibolite facies; the garnet isograd is crossed 1.5 kilometers south of the deposit and the staurolite isograd is located ~1 km further south (Fig.1).

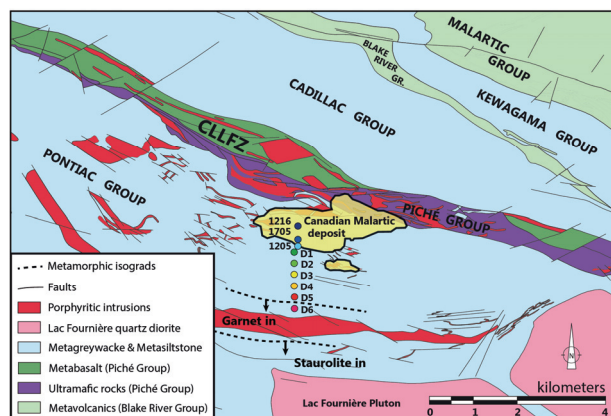


Figure 1. Main lithological units and structural features of the Malartic district (modified from Pilote, 2013 and Sansfaçon, 1987). Dots represent sampled drill holes.

2 Gold mineralization and alteration

2.1 Ore-stage veinlets and alteration

Most gold mineralization occurs in thin quartz-biotite-calcite-microcline±pyrite veinlets with biotite (±microcline-calcite-pyrite) selvages, and in zones of pervasive alteration (Helt et al. 2014). In all rock types, gold mineralization is associated with pyritisation, and potassic/carbonate alteration. The gold mineralization comprises fine-grained native gold and minor tellurides (e.g., petzite, calaverite), usually associated with pyrite.

2.2 Structures

The gold mineralization occurs in elongated, lens-shaped orebodies (Fig.2), controlled by two structures, which are interpreted to be the main fluid pathways (identified by intense hydrothermal alteration and local brecciation):

(1) The E-W trending Sladen Fault marks the contact between metasediments and the main porphyry stock. It extends eastward along the contact between the Piché and Pontiac groups. It is a ductile-brittle shear zone characterised by mylonites overprinted by cataclasites.

(2) The NW-SE pattern of deformation zones consists of asymmetric S-folds (and faulted folds) with long limbs striking approximately E-W, and short limbs striking N-S (R. Sansfaçon 1987; Trudel et al. 1989).

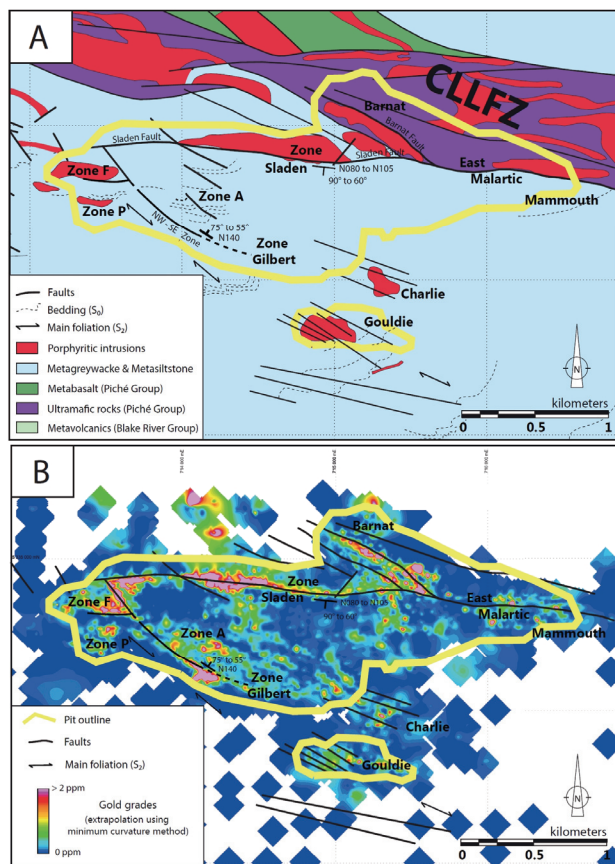


Figure 2. **A.** A lithological/structural map of the Canadian Malartic deposit; **B.** Gold grades and structures that acted as the main hydrothermal conduits for the mineralizing fluids. (**A** modified from Sansfaçon et al. 1987; Trudel et al. 1989, and Pilote 2013; **B** from Canadian Malartic Corporation data and field mapping during our study).

2.3 Alteration zoning

Proximal alteration (usually a few meters to a few tens of meters wide) is dominated by K-feldspar (microcline) and biotite (Mg-rich) and is referred to as potassic alteration. This alteration grades into a transitional potassic-sericitic-calcitic-pyritic alteration shell (tens to hundreds of meters wide) with relatively abundant biotite, white mica, carbonates, and pyrite (the alteration intensity is controlled by the abundance of mineralized veinlets). This transition likely reflects a change in physico-chemical conditions (e.g., a cooling trend) away from the main hydrothermal conduits.

3 Mica mineralogy

3.1 Mode of occurrence

In mineralized zones, hydrothermal biotite and white mica generally occur as fine-grained, shreddy crystals disseminated in the groundmass. Hydrothermal biotite also forms stringers associated with pyrite, and crystallized in pyrite pressure shadows (syn-D₂ deformation). Metamorphic biotite from the alteration halo is lighter colored and more elongated, marking the main foliation, S₂, together with white mica (depending on the nature of the protolith).

3.2 White mica chemistry

White mica in the metasedimentary rocks exhibits a chemical gradient from the deposit toward distal parts of the alteration halo (higher metamorphic grade). There is a steady trend from phengitic muscovite toward end-member muscovite southwards from the deposit, which is indicated by a progressive increase in Al and decreases in Si and Fe+Mg contents. White mica from the deposit has higher Fe and Mg concentrations (phengitic muscovite) than distal white mica, but hydrothermal and metamorphic white micas cannot be distinguished solely on the basis of Fe/(Fe+Mg).

3.3 Biotite chemistry

Hydrothermal biotite can be distinguished from metamorphic biotite by high-Mg (2.9 to 3.3 apfu) and low-Fe (1.6 to 1.9 apfu) concentrations in the former. The low-Fe content of the hydrothermal biotite may be related to the concurrent crystallization of pyrite from the mineralizing fluid. Metamorphic biotite is comparatively Mg-poor (2.2 to 2.8 apfu) and Fe-rich (2.0 to 2.6 apfu) (Fig.3). The extent of hydrothermal biotite is spatially limited, reflecting a sharp decrease of alteration intensity away from the main hydrothermal pathways.

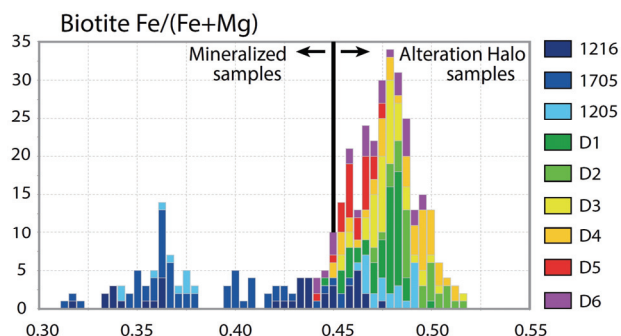
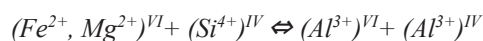


Figure 3. The distribution of molar Fe/(Fe+Mg) in biotite from DDH 1216 to D6 (see Fig.1 for locations). Two distinctly different populations are evident, hydrothermal (deposit) and metamorphic (alteration halo).

3.4 Substitution mechanisms

One of the principal mechanisms controlling the chemical variations in the composition of white mica is the Tschermak substitution:



The contribution of the Tschermak substitution to the compositional variation of mica in the Canadian Malartic deposit was estimated by plotting the sum of Si and divalent elements (e.g., Fe and Mg) against total Al. In the case of the white mica, there is a perfect correlation for (Fe+Mg+Si) vs. total Al ($r^2=0.99$), which corresponds to the slope of the ideal Tschermak substitution line ($y=-x$). The corresponding data for biotite (Fig.4) are also strongly correlated ($r^2=0.74$), although there is a higher degree of scattering than for the white mica because of the involvement of other elements in the Tschermak substitution (e.g., Ti, Mn).

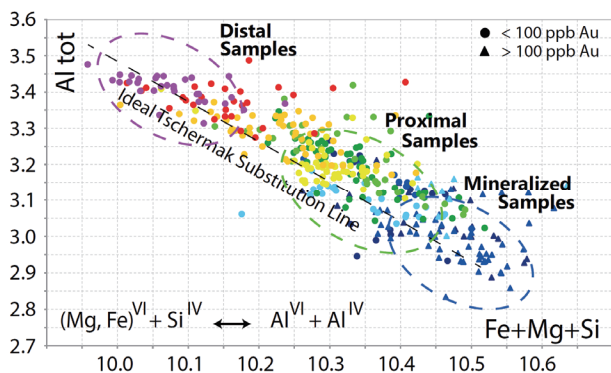


Figure 4. Total Al vs. Fe+Mg+Si (apfu) of biotite compared to the ideal Tschermaak substitution line. The distribution of the data indicates that the extent of the Tschermaak substitution increased with increasing metamorphic grade (same colour scale as for Fig.1 and 3)

3.5 Biotite-white mica element partitioning

The partitioning of major elements between coexisting biotite and white mica was investigated for a series of metasedimentary samples from the mineralized zones (greenschist facies) to distal parts of the alteration halo (amphibolite facies). The muscovite-biotite linear distributions of Al ($r^2=0.87$, Fig.5), K ($r^2=0.71$), Na ($r^2=0.69$), and Si ($r^2=0.60$) indicate that there was little or no influence of variable gradients in external parameters (pressure, temperature, rock composition, oxidation state) on the partitioning of these elements.

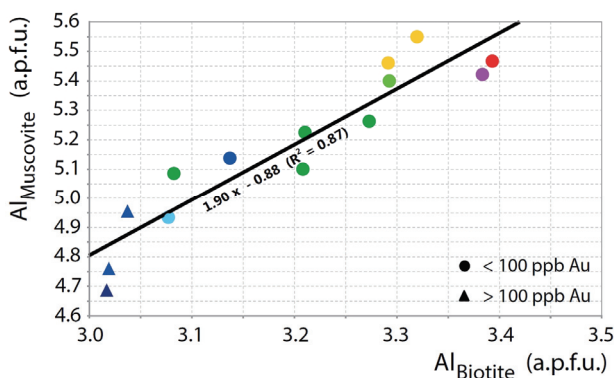


Figure 5. The concentration of Al (apfu) in muscovite versus that in biotite. The linear trend ($r^2 = 0.87$) indicates that partitioning of Al between the two micas was not influenced by variable gradients in external parameters (same colour scale as for Fig.1 and 3)

Interestingly, the partition coefficients of some elements for which their distribution between biotite and white mica is non-linear, *e.g.*, Fe or Mg, appear to increase linearly with distance southwards from the mineralized zones (Fig.6). The partition coefficients of Fe and Mg (D_{Fe}^* and D_{Mg}^* , respectively) are correlated positively with distance from the ore zone ($r^2=0.85$ and 0.60 , respectively), suggesting that partitioning of these elements between the two micas varied with metamorphic grade (which increases southwards) and depended on parameters such as temperature and pressure, or perhaps reflect compositional effects (*e.g.*, higher Al content, Fig. 4).

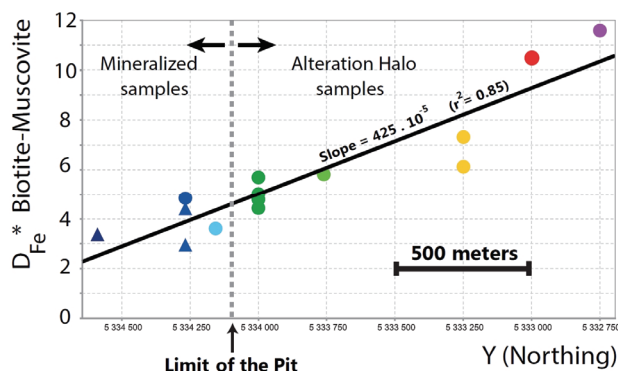


Figure 6. The partition coefficient for Fe between biotite and white mica (D_{Fe}^*) as a function of distance southwards from the mineralized zones (same colour scale as for Fig.1 and 3).

4 Mass changes

4.1 Single precursor

A subset of 145 metasediment samples (greywacke and siltstone) from DDH CM07-1216 (in the mineralized zone) to CD08-D6 (southernmost drillhole) (see Fig.1) was investigated to assess geochemical variations associated with mineralization and hydrothermal alteration. Despite an expected primary compositional variability in the protolith composition (*e.g.*, through graded bedding, source variability), metaturbidities of the Pontiac Group define an apparently cogenetic suite when plotted on a Al_2O_3 - TiO_2 bivariate diagram (MacLean and Barrett 1993).

4.2 Method

Mass changes were evaluated by comparing hydrothermally altered rocks to their least altered equivalent. Immobile elements ratios were used to assess overall mass changes (MacLean 1990)

Least altered samples were selected based on petrographic (color, texture and mineralogy) and geochemical characteristics. As the gold mineralization is associated intimately with pyritization and carbonation of the host rock, the least altered samples were deemed to be rocks with low loss on ignition ($LOI \leq 2$ wt. %) and low Au (≤ 20 ppb), S (≤ 0.3 wt. %) and C (≤ 0.3 wt. %) contents. Distance to the ore shell was also taken into account with the least-altered samples ($n=7$) being selected from the most distal drill holes (D5 and D6, Fig.1).

4.3 Results

Major elements such as K, Na, Ca show pronounced gains for samples from the ore shell (the same is true for LOI), consistent with the mineralogy of the alteration assemblage. The trace elements associated with mineralization (*e.g.*, As, W, Pb, Cd, Te and Ag) as well as C and S also show strong mass gains (several orders of magnitude) compared to least altered equivalents. More particularly, Mo and Sb display steadily decreasing concentration toward the distal parts of the alteration halo (Fig.7).

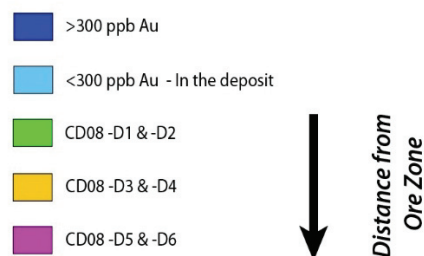
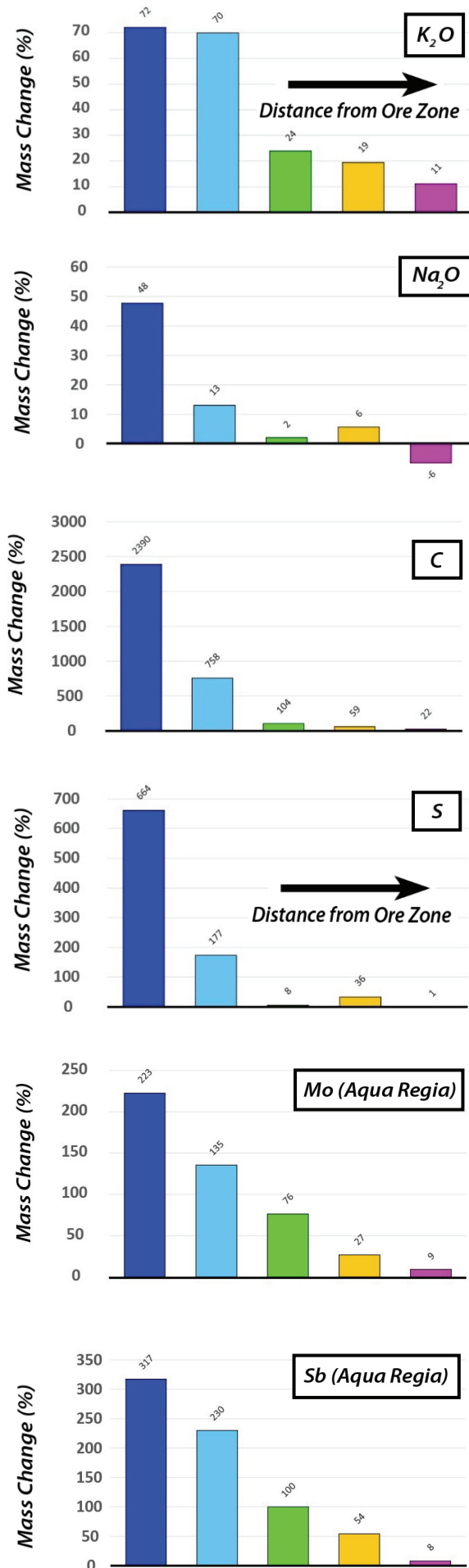


Figure 7. Bar charts illustrating average mass changes (in %, for altered rocks, relative to least altered rocks) in metasediments from the Canadian Malartic deposit and its halo. Samples were separated into five groups, according to their gold content and location: (1) >300ppb (in the deposit); (2) <300 ppb, in the deposit; (3) proximal halo (D1 and D2); (4) medial halo (D3 and D4) and (5) distal halo (D5 and D6) (See Fig.1 for locations).

These results provide a context for further evaluation of the geochemical alteration halo around the Canadian Malartic hydrothermal system. Future work will investigate the controls (alteration, protolith) on and spatial variability of geochemical signatures (from drill hole to district scale).

Acknowledgements

Financial support for the research was provided by grants from CMIC, NSERC (CRD) and SEG. Canadian Malartic Corporation (CMC) afforded access to the field area, drill core, data and internal reports, and made company geologist, F. Bouchard, available for assistance and advice. N. Piette-Lauzière and T. Raskevicius assisted in the field work. "CMIC-NSERC Exploration Footprints Network Contribution 047"

References

De Souza S, Dubé B, McNicoll V, Dupuis C, Mercier-Langevin P, Kjarsgaard K (2014) The world-class Canadian Malartic deposit: a multi-stage porphyry-associated low-grade - bulk-tonnage Archean gold deposit, Southern Abitibi, Québec. Earth Sciences Sector, Contribution Series 20140202, Society of Economic Geologists

Goldfarb RJ, Baker T, Dubé B, Groves DI, Hart CJR, Gosselin (2005) Distribution, character, and genesis of gold deposits in metamorphic terranes. Economic Geology 100th Anniversary Volume 407-450.

Helt KM, Williams-Jones AE, Clark JR, Wing BA, Wares RP (2014) Constraints on the genesis of the Archean oxidized, intrusion-related Canadian Malartic gold deposit, Quebec, Canada. Econ Geol 1209:713-735

MacLean WH (1990). Mass change calculations in altered rock series. Miner Deposita 25:44-49

MacLean WH, Barrett TJ (1993) Lithochemical techniques using immobile elements. Journal of Geochemical Exploration 48:109-133

Pilote P (2013) Carte géologique du district de Malartic, Feuillet 32D01, SIGEOM

Sansfaçon R, Grant M, Trudel P (1987) Géologie de la mine Barnat - Sladen Malartic - District de Val d'Or - Direction Générale de l'Exploration Géologique et Minérale, MB 87-41

Trudel P, Sauvé P (1989) Métallogénie de l'or dans le secteur de Malartic, état des connaissances - Direction Générale de l'Exploration Géologique et Minérale, MB 89-10